Research Paper

Improved Tumor Targeting and Longer Retention Time of NIR Fluorescent Probes Using Bioorthogonal Chemistry

Xianghan Zhang[1], Bo Wang[1], Na Zhao[1], Zuhong Tian[3], Yunpeng Dai[1], Yongzhan Nie[3], Jie Tian[1, 2], Zhongliang Wang[1✉], and Xiaoyuan Chen[4]

1. Engineering Research Center of Molecular-imaging and Neuro-imaging of ministry of education, School of Life Science and Technology, Xidian University, Xi'an, Shaanxi 710026, China;
2. Institute of Automation, Chinese Academy of Sciences, Beijing 100190, China;
3. Institute of Digestive Diseases, Xijing Hospital, Fourth Military Medical University, Xi'an, Shaanxi 710032, China;
4. Laboratory of Molecular Imaging and Nanomedicine, National Institute of Biomedical Imaging and Bioengineering, National Institutes of Health, Bethesda, Maryland, 20892 USA.

✉ Corresponding author: Zhongliang Wang, Email: wangzl@xidian.edu.cn

Abstract

The traditional labeling method for targeted NIR fluorescence probes requires directly covalent-bonded conjugation of targeting domains and fluorophores *in vitro*. Although this strategy works well, it is not sufficient for detecting or treating cancers *in vivo*, due to steric hindrance effects that relatively large fluorophore molecules exert on the configurations and physiological functions of specific targeting domains. The copper-free, "click-chemistry"-assisted assembly of small molecules in living systems may enhance tumor accumulation of fluorescence probes by improving the binding affinities of the targeting factors. Here, we employed a vascular homing peptide, GEBP11, as a targeting factor for gastric tumors, and we demonstrate its effectiveness for *in vivo* imaging via click-chemistry-mediated conjugation with fluorescence molecules in tumor xenograft mouse models. This strategy showed higher binding affinities than those of the traditional conjugation method, and our results showed that the tumor accumulation of click-chemistry-mediated probes are 11-fold higher than that of directly labeled probes. The tracking life was prolonged by 12-fold, and uptake of the probes into the kidney was reduced by 6.5-fold. For lesion tumors of different sizes, click-chemistry-mediated probes can achieve sufficient signal-to-background ratios (3.5–5) for *in vivo* detection, and with diagnostic sensitivity approximately 3.5 times that of traditional labeling probes. The click-chemistry-assisted detection strategy utilizes the advantages of "small molecule" probes while not perturbing their physiological functions; this enables tumor detection with high sensitivity and specific selectivity.

Key words: click chemistry, NIR fluorescence probes, GEBP11, gastric cancer.

Introduction

Near-infrared (NIR) fluorescent imaging has been extensively applied in cancer diagnostics and imaging-guided surgeries due to its relatively low autofluorescence, deep photon penetration, and high sensitivity without risk of radiation exposure [1-4]. NIR imaging technology is still strongly dependent on NIR fluorescent probes; for example, to visualize certain cancer cell types *in vivo* using NIR imaging at the molecular level, tumor-targeting NIR probes are indispensable [5-11]. To date, almost all targeted probes require covalent linking of a targeting moiety (i.e., peptides, antibodies, DNA/RNA aptamers) to an NIR fluorophore molecule (such as an organic dye), using various bioconjugation strategies [1, 12].

However, NIR fluorophores are relatively large molecules (~1kDa) and may have great effects on the steric configurations of tumor-targeting moieties; they may compromise the binding affinities and bioavailability of the targeted probes, may decrease detection sensitivities, and may shorten retention time of the probes in the tumors. Furthermore, to achieve tumor detection with high sensitivity, high doses of the targeting probes have traditionally been used, which unavoidably has incurred toxicity. Therefore, it is desirable to develop a simple, robust strategy that can effectively improve the binding efficiencies of probes and their sensitivities for detecting tumors.

In this study, a new strategy that employs pre-targeting and bioorthogonal conjugate chemistry was present. Targeting domain molecules were first administered into mammalian systems by allowing time for localization in target organs and time for clearance from nontarget organs. Fluorescent coupling partners were then systematically administered, and were conjugated—in a highly selectively manner—with targeted domains *via* rapid bioorthogonal chemical reactions [13, 14]. The inverse-electron-demand Diels-Alder reaction between *trans*-cyclooctene (TCO) and tetrazine (Tz)[15-19] is one example of a fast, highly selective, copper-free, bioorthogonal coupling reaction; this reaction has been widely used in many biological applications for tagging and imaging biomolecules, both in cells and *in vivo* [17, 20-25]. In particular, the introduction of smaller "click-chemistry" moieties (< 0.2 kDa) into targeting domains and fluorescent partners greatly reduces interference with the binding affinities of the specific targeting factors, and even improves their binding efficiencies. This strategy could provide a readout system with low background and high signal output. We reasoned that our strategy could overcome obstacles that have limited the effectiveness of traditional conjugation methods, and could result in more efficient targeting, more prolonged retention of probes, and higher detection sensitivities.

To evaluate and prove this concept, GEBP11—a vascular-homing, cyclic peptide consisting of nine amino acids (CTKNSYLMC)—was chosen as a targeting domain for making highly sensitive diagnoses of gastric cancer. It is well known that angiogenesis and vasculature play important roles in new blood vessel formation during tumor growth [25, 26]. Tumor blood vessels overexpress specific cell surface biomarkers, which does not occur in the blood vessels of normal tissues. The GEBP11 peptide is capable of homing directly to the neovasculature of human gastric cancer tumors, and GEBP11 peptide receptors are expressed at high levels in the cellular membrane and cytoplasm of these tissues [27-29]. In this study, we developed a targeting strategy to visualize gastric cancer *in vitro* and *in vivo* using a novel, GEBP11-based fluorescent probe (Figure 1) consisting of two click-chemistry-mediated components: 1) the pre-labeling agent, GEBP11-TCO, and 2) the NIR fluorescent agent, cyanine-5.5 (Cy5.5)-Tz. Compared to traditional covalent conjugation probes (e.g., GEBP11-Cy5.5), click-chemistry-mediated probes exhibit higher binding affinity, more efficient targeting, enhanced detection sensitivity, and prolonged retention time.

Materials and Methods

Materials and Measurements

All solvents and starting materials were purchased commercially (TCI Shanghai, J&K, Sigma-Aldrich) and used without further purification. The TCO-NHS was commercially available from Click Chemistry Tools. The GEBP11 peptide was supplied by the State Key Laboratory of Cancer Biology, the Institute of Digestive Diseases, Xijing Hospital, and the Fourth Military Medical University.

The high-performance liquid chromatography (HPLC) was used for purification of probes by on a Waters prep LC 2545 instrument. ESI-TOF-MS spectra measurements were performed by a Bruker QTOF II mass spectrometer. The imaging experiments *in vitro* were recorded on an Olympus FV 10i confocal fluorescent microscope. *In vivo* fluorescence imaging analysis was carried out in an IVIS Kinetic imaging system. The binding affinity was detected with a BD Accuri C6 flow cytometry.

A detailed description of the synthesis and characterization of all compounds can be found in the Supplementary Materials.

In Vitro Fluorescence Imaging

The cell lines including SGC-7901 and GES cells were dissociated using 0.5% trypsin-EDTA when grown with 80% confluence and suspended in fresh medium. Almost 1×10^5 cells were plated in a MillicellR EZSLIDE well and cultured overnight. The cells were pre-incubated with 5 μM GEBP11-TCO or GEBP11 for 3 h at 37 °C and then incubated with 5 μM Cy5.5-Tz for 0.5 h. After that, the cells were washed with PBS three times. The cells were incubated with 5 μM GEBP11-Cy5.5 for 0.5 h at 37 °C and washed with PBS three times. In the blocking experiment, the SGC-7901 cells were pretreatment with unlabeled GEBP11 for 3 h at 37 °C and followed by 5 μM GEBP11-TCO for 3 h, then incubated with 5 μM Cy5.5-Tz for 0.5 h. After incubation, the cells were washed with PBS to replace the medium, fixed with 4% paraformaldehyde fixative for 10 min, washed

with PBS two times. For the nuclear staining, 10 μg/mL 4'6-Diamidino-2-phenylindole (DAPI) was used for 5 min at room temperature. The coverslips were examined on confocal laser microscopy and images were acquired at 60 × magnification.

Measurement of binding affinity

The binding affinity of the probes to the SGC-7901 cells was determined using a constant number of cells and measuring the fluorescence intensity as the concentration of bound peptide increased to saturation. The probes were serially diluted in 1640 culture medium at concentrations that varied from 0 to 80 μM, and incubated with 10^6 cells in 12-well plates on ice. For click group, the cells were pre-incubated with with 5 μM GEBP11-TCO for 5 h and incubated with Cy5.5-Tz for 3 h on ice. For GEBP11-Cy5.5 group, the cells were incubated with GEBP11-Cy5.5 for 3 h on ice. The cells were washed with ice-cold PBS three times to remove the unbound

probes. The samples were digested with trypsin and harvested for flow cytometry analysis with 640 nm emission.

Tumor Xenograft

The 6-week-old male athymic nude mice which weight was 20 – 25 g were supplied by the Animal Center of the Fourth Military Medical University (FMMU). Human gastric carcinoma xenografts were induced by subcutaneous injection of 5×10^6 gastric carcinoma cells SGC-7901 into the upper limb per mouse. When the diameter of subcutaneous tumor developed to approximately 4.3 ± 0.3 mm or 8.4 ± 0.5 mm, *in vivo* imaging was recorded at different time after intravenous injection of click, non-click, Cy5.5-GEBP11 groups via tail vein using PerkinElmer IVIS imaging system. The animal use was approved by the Institutional Animal Care and Use Committee of the Fourth Military Medical University.
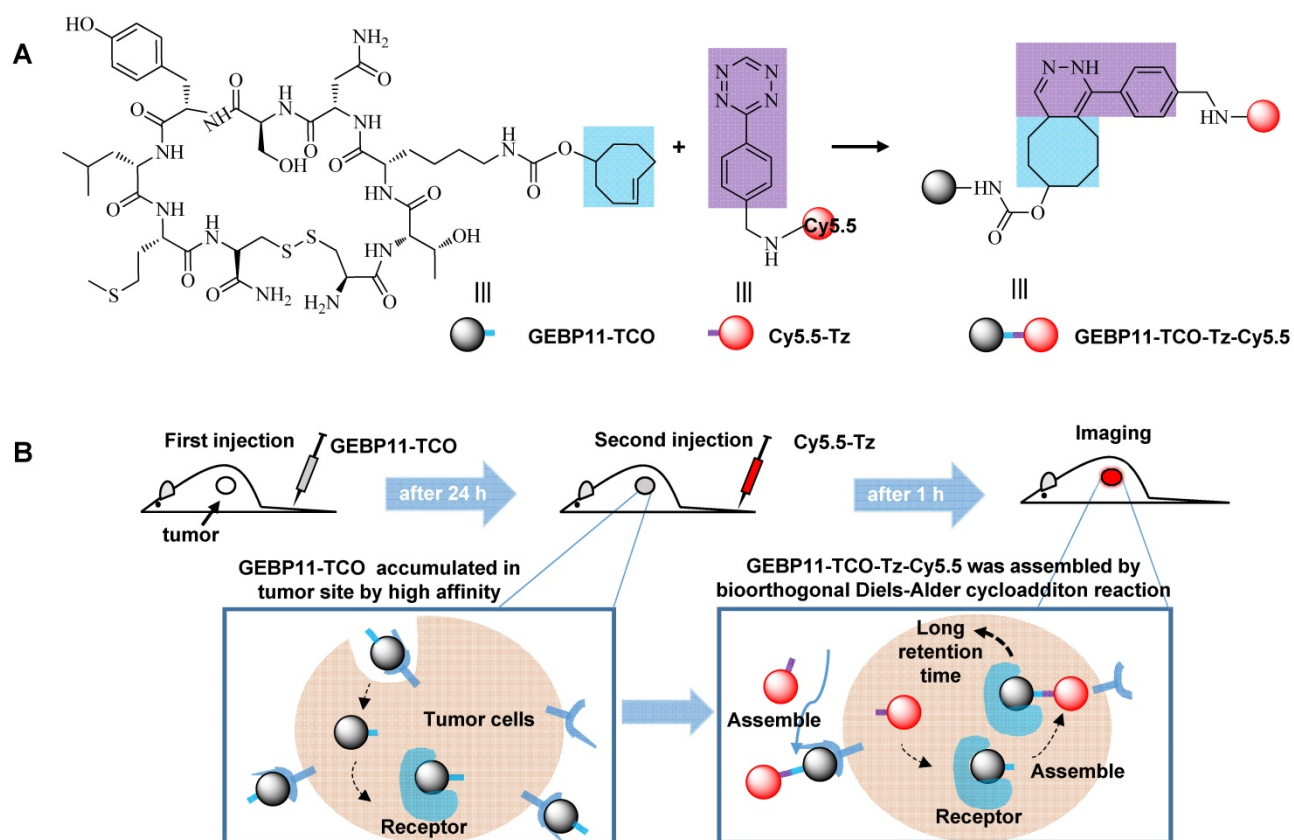
Figure 1. Illustration of the mechanism of *in vivo* imaging by Click-mediated GEBP11 probes in human tumor xenograft mouse models. (A) Bioorthogonal inverse electron-demand Diels-Alder (IED-DA) reaction between TCO and Tz. Blue, the trans-cyclooctene group (TCO); purple, the tetrazine group (Tz); dark, the vascular homing targeting peptide GEBP11; red, NIR fluorophore Cy5.5. (B) Mice are treated first with GEBP11-TCO and then reacted with Cy5.5-Tz.

In vivo Fluorescence Imaging and Imaging Data Analysis

For the click and non-click treatment groups, mice were injected with GEBP11-TCO or GEBP11 24 h prior to injection with Cy5.5-Tz. Mice in directly labeling group were injected with Cy5.5-GEBP11 immediately prior to imaging. Competitive click controls were preinjected with GEBP11-TCO 3h prior to injection with Cy5.5-Tz, and the competitive blocking groups were preinjected with GEBP11 5 h, pre-injected with GEBP11-TCO 3 h, injected with Cy5.5-Tz immediately prior to imaging. Mice were anesthetized with 5% isofluorane and then transferred to the IVIS imaging system. After imaging experiments, the mice were killed by cervical dislocation, and the organs were harvested for imaging. Image fluorescence intensity data were quantified by region-of-interest (ROI) measurement using Living Image software 4.5.1 (IVIS). All imaging times were starting from the injection of Cy5.5-Tz or GEBP11-Cy5.5, which could ensure the unity of the exposure time of fluorescent signals from Cy5.5.

Biodistribution and Statistics

Mice bearing SGC-7901 tumors were injected with 4 nmol probes in 200 μL saline. At 24 HPI, mice were euthanized and tissue was collected for weighing. The linear correlation of fluorescence intensity and concentrations, and the relations of weigh and volume were used to determine the biodistribution of probes in the organs. All of ROI data was done to subtract the tissue autoflorescence. Signal-to-background was calculated by [(tumor ROI – mean background ROI) / mean background ROI], mean background ROI = (back ROI + lower limb ROI + abdomen ROI)/3. All statistical analysis of two-sample comparisons was performed using the two-way Student's t-test.

Results and Discussion

Preparation of GEBP11-TCO, Cy5.5-Tz, and GEBP11-Cy5.5

The TCO-conjugated peptide (GEBP11-TCO) was prepared by coupling (*E*)-cyclooct-4-enyl-2,5-dioxopyrrolidin-1-yl carbonate (TCO-NHS) with GEBP11. A crude white solid was obtained by adding ethyl acetate to this mixture and then washing with ether three times. After purification using a pre-HPLC, an 80% yield was obtained. Tetrazine-conjugated cyanine 5.5 (Cy5.5-Tz) and GEBP11-conjugated cyanine 5.5 (GEBP11-Cy5.5) were synthesized by coupling Cy5.5-NHS with either tetrazine or GEBP11 at room temperature. After pre-HPLC, the Cy5.5-Tz and GEBP11-Cy5.5 products

were obtained at yields of 90% and 75%, respectively. All of the products were confirmed using high-resolution mass spectrometry (HRMS; ESI, Figure S1 and S2) and were stable at –20 °C for more than eight months.

### *In vitro* specific selectivity of probes to gastric tumor cells

The low cytotoxicity is a prerequisite for the clinical application of the fluorescent probes. The cytotoxicity of the click, GEBP11-Cy5.5 and Cy5.5-Tz probes were determined using the HCA protocol. As shown in Figure S3, the cells exhibited good proliferative ability after being treated with all the probes even at the highest concentrations over 24 h, indicating the probes had no significant cytotoxicity to cells. To evaluate whether GEBP11 combined with NIR imaging technology *via* the click-chemical reaction approach could selectively image gastric tumor cells, the gastric cancer cell line SGC-7901 and the immortalized fetal gastric epithelial cell line GES were chosen for use. Cells were pretargeted with 5 μM of either GEBP11-TCO (designated as the "click-mediated" group) or GEBP11 (the "non-click" group) for 3 h, then were treated with 5 μM of Cy5.5-Tz for 0.5 h, and were then visualized using confocal laser microscopy and flow cytometry (Figure 2). Treatment of the SGC-7901 cells with the click-mediated probes led to clear, extremely bright red signals at cellular cytoplasmic regions.

Flow cytometric analyses demonstrated that the binding percentages of click-mediated probes to SGC-7901 cells were nearly 3-fold higher (86.4 % *vs.* 29.1%) than those of non-click probes (GEBP11/Cy5.5-Tz). Weak fluorescence of SGC-7901 cells after incubation with non-click probes suggested thenon-specific cell permeability of Cy5.5. By contrast, the treatment of GES cells with both click and non-click probes showed very weak fluorescence signals (Figure S4). *In vitro* blocking experiments were also performed to evaluate the specificity of click-mediated probes. SGC-7901 cells were pretreated with 5 μM of GEBP11 for 3 h and were then incubated sequentially with GEBP11-TCO (3 h) and Cy5.5-Tz (0.5 h); fluorescence signal strength and the binding percentages of the probes to the cells clearly decreased. Flow cytometric analyses showed that, compared to blocking cells, the binding percentages of unblocking cells were about 3.7-fold higher (86.4% *vs.* 23.5%). Therefore, click-mediated GEBP11 fluorescent probes were able to selectively differentiate gastric tumor cells from normal cells.

We wondered if directly labeled probes (such as GEBP11-Cy5.5) affect the efficiency with which the targeting factors can target the cells. To determine

this, GEBP11-Cy5.5 probes were used to stain SGC-7901 cells for 0.5 h; as can be seen in Figure 2, the fluorescent signal of GEBP11-Cy5.5 was much lower than that of GEBP11-TCO/Tz-Cy5.5 (with binding percentages of 30.2% and 86.4%, respectively). We hypothesized that the lower binding affinities of GEBP11-Cy5.5 probes to SGC-7901 cells could be due to interference (in the form of steric hindrance) caused by the Cy5.5 molecules. Because of the similar molecular weight and molecular size of Cy5.5 (913 Da) with GEBP11 (1,058 Da), Cy5.5 would impact the steric configuration of the GEBP11 peptide, and would perturb its physiological functions. By contrast, TCO agents are five-fold smaller in molecular weight

(170 Da) and have fewer effects on the tumor-targeting properties of GEBP11. To confirm this hypothesis, the cells were incubated with both categories of probe at 4 °C to investigate their respective tumor cell-targeting efficacies. As shown in Figure S5, the click probes exhibited an apparent dissociation constant (K_d) of 32.10 μM, while the traditional probes had a K_d of 54.49 μM. This indicated that click-mediated GEBP11 probes showed higher binding affinities to their targets due to the reduced targeting ability of GEBP11 after Cy5.5 conjugation. The steric interference from the fluorophore molecules had a striking effect on the targeting properties of the GEBP11 peptide.
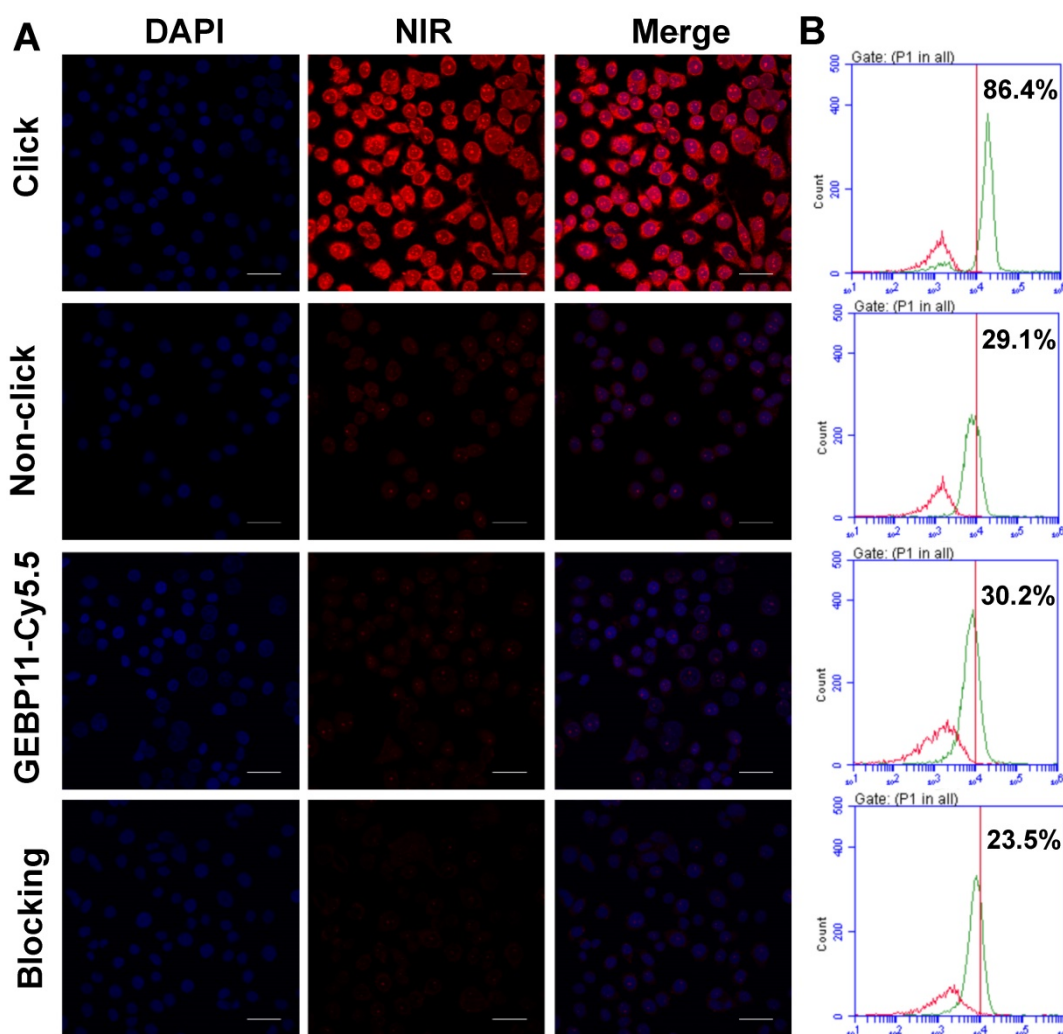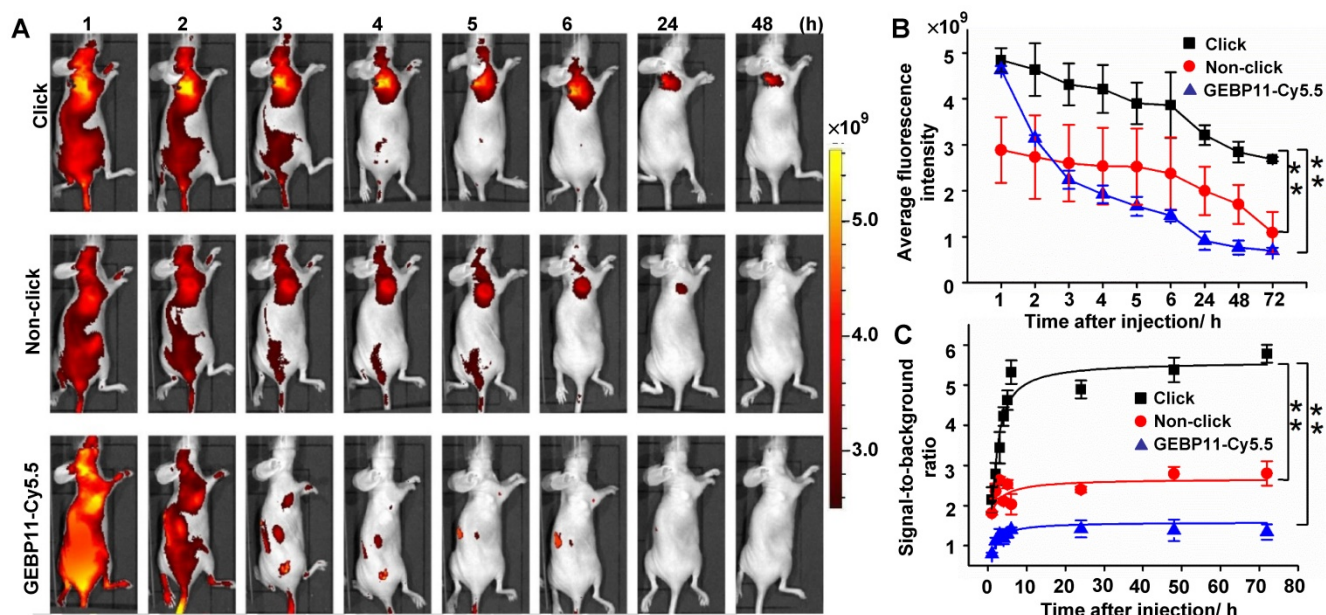

Figure 2. Binding affinity of click, non-click or GEBP11-Cy5.5 probes *in vitro*. (A) Fluorescence microscopy imaging of SGC-7901 cells labeled with click probes (pre-labeled with 5 μM GEBP11-TCO for 3 h, followed by 5 μM Cy5.5-Tz), non-click probes (pre-labeled with 5 μM GEBP11 for 3 h, followed by 5 μM Cy5.5-Tz), GEBP11-Cy5.5 (5 μM) and blocking probes (pre-labeled with 5 μM GEBP11 for 3 h, followed by 5 μM click probes). Cells were stained with nuclear dye DAPI (blue) and the NIR dye Cy5.5 (red). All of the images were acquired at 60× magnification. The scale bar represents 30 μm. (B) Representative histograms from flow-cytometric analysis binding to SGC-7901 cells of labeled (green) and non-labeled (red).

In vivo NIR fluorescent imaging

To better understand the kinetics of the click-chemistry-mediated probes *in vivo*, target region-of-interest (ROI) signals from tumors were evaluated, as shown in Figure S6. Tumor uptake of the click-mediated probes reached a maximum at 0.5 hours post-injection (HPI), and tumors displayed a 220% net increase in fluorescence intensity during this time period. We also investigated the specificities, binding affinities, and clearance rates of the three probe labeling groups in terms of *in vivo* behavioral criteria (pharmacokinetics and intratumor distribution), which we validated by profiling their biodistributions.

NIR fluorescence imaging *in vivo* was assessed using intravenous injections of 4 nmol of click-mediated GEBP11, non-click-mediated GEBP11, or GEBP11-Cy5.5 probes, in female nude mice bearing SGC-7901 subcutaneous xenograft models (Figure 3). The net accumulation of each probe within tumors was determined by subtracting the mean ROI signal of untreated mice from the tumor signal of treated mice. We found that the fluorescence signals from click probe groups were significantly brighter than those of the non-click probe or GEBP11-Cy5.5 groups (Figure 3B), and these brighter signals constituted the most remarkable difference amongst the three groups. By 6 HPI, the signal-to-background ratios in the click probe groups were 2.6 and 3.8 times those of the non-click and GEBP11-Cy5.5 probe groups, respectively (Figure 3C). A 3.5-fold increase in the signal-to-background ratio in the click groups *vs.* the GEBP11-Cy5.5 group occurred at 24 HPI; over a period of continuous signal enhancement, this value increased to 4-fold at 72 HPI. Of note, the tumors that were stained with the click groups maintained fluorescent signals for up to 72 HPI, indicating that the long retention time of the click-mediated probes would probably allow for long-term *in vivo* tracking. By contrast, the GEBP11-Cy5.5 groups displayed barely detectable signals from tumors at 6 HPI, constituting a probe tracking life that was 12-fold shorter than that of the click-mediated probes. Longer retention time of click-mediated GEBP11 probes could be ascribed to the higher binding affinities to their targets. In addition, to further verify the longer retention time of click-mediated probes, we investigated the urine excretion by collecting urine after intravenous injection of the probes. As shown in Figure S7, pharmacokinetics of click-mediated probes demonstrated slower urine excretion than that of GEBP11-Cy5.5 through the renal system, indicating the longer retention time of click-mediated probes. All together, click-mediated probes were able to produce higher tumor accumulations, longer retention time, and significant fluorescence enhancements when compared to traditional probes.

Figure 3. Targeting specificity of click, non-click or GEBP11-Cy5.5 probes *in vivo* imaging. (A) Fluorescence imaging of subcutaneous tumor-bearing nude mice after intravenous injection with probes. Click group: pre-injected with 8 nmol GEBP11-TCO for 24 h, and then injected with 4 nmol Cy5.5-Tz. Non-click group: injected with 8 nmol GEBP11 for 24 h, and then 4 nmol Cy5.5-Tz. GEBP11-Cy5.5 group: 4 nmol GEBP11-Cy5.5. (B) Average fluorescence signal emitted from the tumor tissue over time. ** $p < 0.01$ between groups indicated by brackets. (C) Signal-to-background ratios over time. ** $p < 0.01$. All the error bars indicate standard deviation from $n = 3$ animals.

To further validate the assessment that click-meditated probes were more specific than the directly labeled probes, RGD peptide was chosen as a targeting factor model to test, and click-meditated RGD probe experiments were then conducted *in vitro* and *in vivo* using NIR fluorescent imaging in the SGC-7901 models, as shown in Figure S8. The results showed that compared with the directly labeled probes, click-meditated probes exhibited more specific selectivity and more intense fluorescence signals. This demonstrates that the click-mediated targeting strategy is robust, and strongly suggests that its effectiveness in improving the selectivity and sensitivity of targeting factors to tumors is universal.

To make a comprehensive assessment of diagnostic sensitivity, signal-to-background ratios were measured at tumor lesions with different sizes (Figure S9). At 6 HPI, the signal contrasts between

tumor sites and normal tissues were maximal, because by that time, most nonspecific binding had washed out. The signal-to-background ratios observed for the click probe groups were 3.3 times greater than those of the GEBP11-Cy5.5 groups for smaller tumor lesions (click *vs*. GEBP11-Cy5.5: [5.25±0.52] *vs*. [1.57±0.40]), and were 3.8-times higher for larger tumor lesions (click *vs*. GEBP11-Cy5.5: [3.70±0.29] *vs*. [0.97±0.35]). This indicated that the click-mediated GEBP11 probe had greatly improved diagnostic sensitivity, and that this enhancement was independent of the tumor size—indicating possibilities for detecting tumors with high specific selectivity and sensitivity.

Biodistribution of click-mediated GEBP11 probes

To better understand the highly specific selectivity and sensitivity of click-mediated probes to tumor lesions, the kinetic data were then cross-validated against the biodistribution of the probes in the organs of the mice. For three probe groups, organs were harvested and imaged after 24 HPI (Figure 4). Compared with the larger GEBP11-Cy5.5 agents, the smaller click probes showed significant differences in pharmacokinetics, as shown in Figs. 4A and B. Click-mediated GEBP11 probes exhibited nearly 5.4-fold greater fluorescence than the directly labeled probe in the tumor site ($p < 0.05$), and showed 6.5-fold less fluorescence in the kidney. This indicated that click-mediated probes show much higher bioavailability than do non-click-mediated probes. Furthermore, when pathological examinations were carried out using hematoxylin and eosin (H&E) microscopy, no obvious structural changes were observed in any organs (Figure S10). There were no detectable side effects, or signs of cytotoxicity, from the click-mediated probes.

To compare the *in vivo* specificity of the three types of probe, tumor-to-organ signal ratios were calculated. Passively targeted fluorescent probes (GEBP11/Tz-Cy5.5) showed higher liver and kidney uptake than the click-mediated probes. The [tumor-to-kidneys] and [tumor-to-liver] signal ratios of the click groups were [14.6±2.57] and [5.92±1.45], respectively, while the corresponding values for GEBP11-Cy5.5 were [0.32±2.84] and [3.99±0.32], respectively (Figs. 4C and
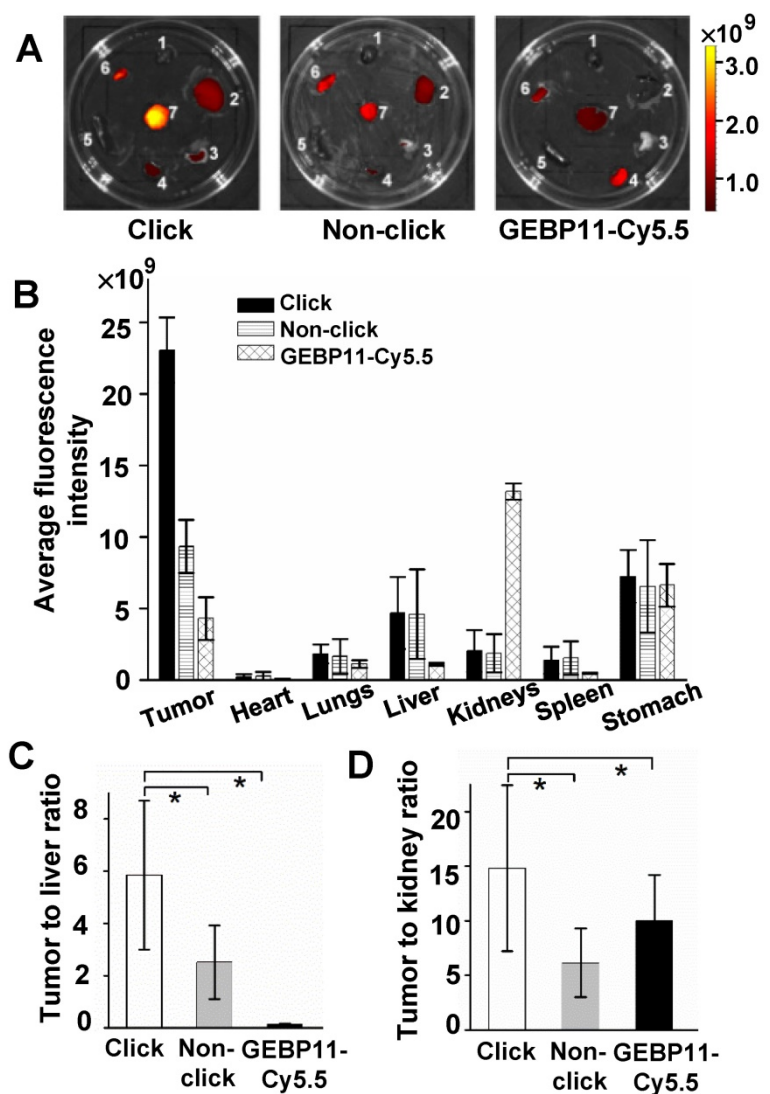
Figure 4. Biodistribution study of click, non-click or GEBP11-Cy5.5 groups at 24 HPI. (A) Fluorescence images of excised organs harvested from mice 24 HPI (1 heart, 2 liver, 3 lungs, 4 kidneys, 5 spleen, 6 stomach, 7 tumor). (B) The fluorescence intensity analysis of excised organs. (C) Tumor-to-liver ratios. * *p* < 0.05, *n* = 3. (D) Tumor-to-kidney ratios. * *p* < 0.05, *n* = 3.

D). The click groups also showed the highest signal contrasts between tumor tissues and non-tumor tissues (Figure S11).

The tumors of the click probe mice group contained 7.2% of the fluorescence dyes at 24 HPI, as measured by linear correlation (Figure S12). This was higher than the 3.6% and 0.68% amounts retained in the mice of the non-click group and GEBP11-Cy5.5 group, respectively. However, the probe uptake rates in the click probe group were about 2 and 11 times higher than those in the non-click group and GEBP11-Cy5.5 group, respectively. It is essential to consider the impacts of molecular weight, size, and steric hindrance of fluorophores on the biological activities of the targeted peptides. It was entirely predictable that the fluorophores may disrupt the binding affinities and biological activities of the targeted peptides, greatly affecting the peptides' transportation into tumor sites and subsequently into tumor cells. The higher tumor uptake of probes in the click group can be attributed to the higher selectivity and rapid bioorthogonal reactions occurring with the click-mediated probes in the tumor tissues. To further confirm our result, we performed the confocal images of tumor tissues. As shown in Figure S13, it was found that click group indeed showed higher fluorescenc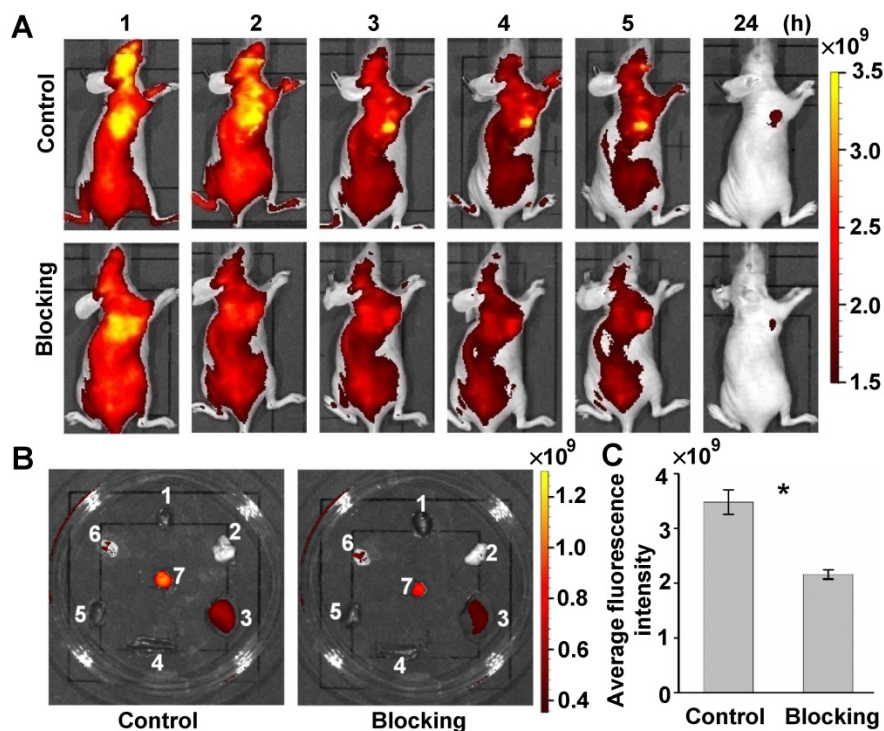e imaging from the cryosectioned tumor tissues than that of GEBP11-Cy5.5 group, indicating higher tumor accumulation of probes in the click group.

To further validate the targeting specificity of the click-mediated GEBP11 probe *in vivo*, a competition blocking experiment was also performed. Control mice were intravenously pre-injected with 8 nmol of GEBP11-TCO for 3h, and then with 4 nmol of Cy5.5-Tz. Blocking experiment mice were first intravenously pre-injected with 8 nmol of unlabeled GEBP11 for 5h, then were sequentially injected with 8 nmol of GEBP11-TCO for 3h, followed by 4 nmol of Cy5.5-Tz. The xenograft mice of both groups were observed over 24 h, as shown in Figure 5A. The fluorescence signal at the tumor sites of mice in the blocking group showed a 41% reduction compared to those in the control mice. Fluorescence images of excised organs indicated that the mice used for blocking inhibition showed nonsignificant reductions of probe accumulation in the liver, spleen, and kidneys (Figure 5B). Quantitative fluorescence signals of tumors *in vivo* were acquired after 4 h from intravenous injection (Figure 5C). By this time, most of the nonspecific binding had washed out in normal tissue. The average fluorescence signal in tumors from control mice was 1.6 times higher than that of the competition blocking mice. However, some residual signals in mice of the blocking experiments were observed. This was perhaps due to the non-specific accumulation of Cy5.5. That is to say, the GEBP11 inhibitor successfully reduced tumor uptake of click-mediated probes when compared to the control group, indicating high specific selectivity of click-mediated probes *in vivo*.

Figure 5. Targeted specificity of GEBP11 peptide performed on the competition blocking experiment *in vivo*. (A) Fluorescence imaging of subcutaneous tumor-bearing nude mice after intravenous injection with probes. Control group: pre-injected with 8 nmol GEBP11-TCO for 3 h, and then 4 nmol Cy5.5-Tz. Blocking group: pre-injected with 8 nmol GEBP11 for 5 h, followed by sequential injection with 8 nmol GEBP11-TCO for 3 h and 4 nmol Cy5.5-Tz. (B) Fluorescence images of tissues harvested from mice 24 HPI (1 heart, 2 lungs, 3 liver, 4 spleen, 5 kidneys, 6 stomach, 7 tumor). (C) Average fluorescence intensity found a higher signal of control group *vs* blocking group at 4 HPI ($n = 3$, * $p < 0.05$).

Conclusions

In summary, we have demonstrated a click-assisted strategy of a vascular homing peptide GEBP11 for highly specific detection of gastric tumor in living animals. Compared with the direct labeling method, the click-chemistry strategy therefore has three clear advantages: 1) enhance tumor accumulation of probes for easy transport of small molecules into tumors, 2) the large agent assembled *via* click chemistry in tumors would reduce clearance

and improves retention, and 3) avoid interference of the physiological function of specific targeting factor by fluorophores. The facile procedure may also be explored for labeling different types of specific factors for detecting tumors or improving tumor delivery of diagnostic and therapeutic agents in living systems.

Acknowledgements

Supplementary Material

Supplementary figures.
http://www.thno.org/v07p3794s1.pdf

Competing Interests

The authors have declared that no competing interest exists.

References

1. Kobayashi H, Ogawa M, Alford R, Choyke PL, Urano Y. New strategies for fluorescent probe design in medical diagnostic imaging. Chemical reviews. 2009; 110: 2620-40.
2. Gao J, Chen K, Xie R, Xie J, Lee S, Cheng Z, et al. Ultrasmall near-infrared non-cadmium quantum dots for in vivo tumor imaging. Small. 2010; 6: 256-61.
3. Hyun H, Park MH, Owens EA, Wada H, Henary M, Handgraaf HJ, et al. Structure-inherent targeting of near-infrared fluorophores for parathyroid and thyroid gland imaging. Nature medicine. 2015; 21: 192-7.
4. Hu Z, Qu Y, Wang K, Zhang X, Zha J, Song T, et al. In vivo nanoparticle-mediated radiopharmaceutical-excited fluorescence molecular imaging. Nature communications. 2015; 6.
5. Burggraaf J, Kamerling IM, Gordon PB, Schrier L, De Kam ML, Kales AJ, et al. Detection of colorectal polyps in humans using an intravenously administered fluorescent peptide targeted against c-Met. Nature medicine. 2015; 21: 955-61.
6. Savariar EN, Felsen CN, Nashi N, Jiang T, Ellies LG, Steinbach P, et al. Real-time in vivo molecular detection of primary tumors and metastases with ratiometric activatable cell-penetrating peptides. Cancer research. 2013; 73: 855-64.
7. Atreya R, Neumann H, Neufert C, Waldner MJ, Billmeier U, Zopf Y, et al. In vivo imaging using fluorescent antibodies to tumor necrosis factor predicts therapeutic response in Crohn's disease. Nature medicine. 2014; 20: 313-8.
8. Vahrmeijer AL, Hutteman M, Van Der Vorst JR, Van De Velde CJ, Frangioni JV. Image-guided cancer surgery using near-infrared fluorescence. Nature reviews Clinical oncology. 2013; 10: 507-18.
9. Chi C, Du Y, Ye J, Kou D, Qiu J, Wang J, et al. Intraoperative imaging-guided cancer surgery: from current fluorescence molecular imaging methods to future multi-modality imaging technology. Theranostics. 2014; 4: 1072-84.
10. Harlaar NJ, Koller M, de Jongh SJ, van Leeuwen BL, Hemmer PH, Kruijff S, et al. Molecular fluorescence-guided surgery of peritoneal carcinomatosis of colorectal origin: a single-centre feasibility study. The Lancet Gastroenterology & Hepatology. 2016; 1: 283-90.
11. Ye Y, Chen X. Integrin targeting for tumor optical imaging. Theranostics. 2011; 1: 102-26.
12. Achilefu S. The Insatiable Quest for Near-Infrared Fluorescent Probes for Molecular Imaging. Angewandte Chemie International Edition. 2010; 49: 9816-8.
13. Tang L, Yin Q, Xu Y, Zhou Q, Cai K, Yen J, et al. Bioorthogonal oxime ligation mediated in vivo cancer targeting. Chemical Science. 2015; 6: 2182-6.
14. Wang H, Wang R, Cai K, He H, Liu Y, Yen J, et al. Selective in vivo metabolic cell-labeling-mediated cancer targeting. Nature Chemical Biology. 2017; 13: 415-24.
15. Devaraj NK, Weissleder R. Biomedical applications of tetrazine cycloadditions. Accounts of chemical research. 2011; 44: 816-27.
16. Jewett JC, Bertozzi CR. Cu-free click cycloaddition reactions in chemical biology. Chemical Society Reviews. 2010; 39: 1272-9.
17. Rossin R, Robillard MS. Pretargeted imaging using bioorthogonal chemistry in mice. Current opinion in chemical biology. 2014; 21: 161-9.
18. Rossin R, Renart Verkerk P, van den Bosch SM, Vulders R, Verel I, Lub J, et al. In vivo chemistry for pretargeted tumor imaging in live mice. Angewandte Chemie International Edition. 2010; 49: 3375-8.
19. Mejia Oneto JM, Khan I, Seebald L, Royzen M. In Vivo Bioorthogonal Chemistry Enables Local Hydrogel and Systemic Pro-Drug To Treat Soft Tissue Sarcoma. ACS Central Science. 2016; 2: 476-82.
20. Devaraj NK, Thurber GM, Keliher EJ, Marinelli B, Weissleder R. Reactive polymer enables efficient in vivo bioorthogonal chemistry. Proceedings of the National Academy of Sciences. 2012; 109: 4762-7.
21. Lang K, Davis L, Torres-Kolbus J, Chou C, Deiters A, Chin JW. Genetically encoded norbornene directs site-specific cellular protein labelling via a rapid bioorthogonal reaction. Nature chemistry. 2012; 4: 298-304.
22. Xie R, Hong S, Chen X. Cell-selective metabolic labeling of biomolecules with bioorthogonal functionalities. Current opinion in chemical biology. 2013; 17: 747-52.
23. Sun Y, Ma X, Cheng K, Wu B, Duan J, Chen H, et al. Strained cyclooctyne as a molecular platform for construction of multimodal imaging probes. Angewandte Chemie International Edition. 2015; 54: 5981-4.
24. Haun JB, Devaraj NK, Hilderbrand SA, Lee H, Weissleder R. Bioorthogonal chemistry amplifies nanoparticle binding and enhances the sensitivity of cell detection. Nature nanotechnology. 2010; 5: 660-5.
25. Chung AS, Lee J, Ferrara N. Targeting the tumour vasculature: insights from physiological angiogenesis. Nature Reviews Cancer. 2010; 10: 505-14.
26. Folkman J. Role of angiogenesis in tumor growth and metastasis. Seminars in oncology. Elsevier; 2002: 15-8.
27. Liang S, Lin T, Ding J, Pan Y, Dang D, Guo C, et al. Screening and identification of vascular-endothelial-cell-specific binding peptide in gastric cancer. Journal of molecular medicine. 2006; 84: 764-73.
28. Zhang J, Hu H, Liang S, Yin J, Hui X, Hu S, et al. Targeted radiotherapy with tumor vascular homing trimeric GEBP11 peptide evaluated by multimodality imaging for gastric cancer. Journal of Controlled Release. 2013; 172: 322-9.
29. Liu L, Yin J, Liu C, Guan G, Shi D, Wang X, et al. In vivo molecular imaging of gastric cancer in human-murine xenograft models with confocal laser endomicroscopy using a tumor vascular homing peptide. Cancer letters. 2015; 356: 891-8.